

(1)

79-0411

AD-A148 631

TR-738  
DAAG-53-76C-0138

March, 1979

TEXTURE CLASSIFICATION USING  
GRAY LEVEL COOCCURRENCE BASED ON EDGE MAXIMACharles R. Dyer  
Tsai-Hong Hong  
Azriel RosenfeldComputer Science Center  
University of Maryland  
College Park, MD 20742APPROVED FOR PUBLIC RELEASE,  
DISTRIBUTION IS UNLIMITED (A)

DTIC  
ELECTE  
DEC 14 1984  
S D  
B

DTIC FILE COPY

UNIVERSITY OF MARYLAND  
COMPUTER SCIENCE CENTERCOLLEGE PARK, MARYLAND  
20742

04 12 06 009

TR-738  
DAAG-53-76C-0138

March, 1979

CSC - TR-738

TEXTURE CLASSIFICATION USING  
GRAY LEVEL COOCCURRENCE BASED ON EDGE MAXIMA

Charles R. Dyer  
Tsai-Hong Hong  
Azriel Rosenfeld

Computer Science Center  
University of Maryland  
College Park, MD 20742

ABSTRACT

This paper introduces a new class of texture features based on the joint occurrences of gray levels at points defined relative to edge maxima. These features are compared with previous types of cooccurrence-based features, and experimental results are presented indicating that the new features should be useful for texture classification.

APPROVED FOR PUBLIC RELEASE;  
DISTRIBUTION IS UNLIMITED (A)

DTIC  
ELECTED  
DEC 14 1984  
S D  
B

The support of the Defense Advanced Research Projects Agency and the U. S. Army Night Vision Laboratory under Contract DAAG-53-76C-0138 (DARPA Order 3206) is gratefully acknowledged, as is the help of Ms. Kathryn Riley in preparing this paper. The authors also wish to thank Dr. David Milgram for his help in the initial stages of this work.

A

Blank Page

## 1. Introduction

Features based on the joint frequencies of occurrence of pairs of gray levels at given separations are often used for texture analysis.<sup>[1]</sup> Recently, Davis et al. <sup>[2-3]</sup> have suggested using joint occurrences of local maxima of a local property (e.g., edge maxima) to define texture features. This paper proposes a hybrid approach using joint gray level occurrences at and near edge maxima. → (to p1473 A (back))

Section 2 reviews the standard cooccurrence approach and Davis' approach, and also describes the proposed new approach. Section 3 presents several sets of experimental results, using the pictures in Figure 7, which indicate that the proposed features should be useful for texture classification.

15

Accession For	
NTIS GRA&I	
DTIC TAB	<input checked="" type="checkbox"/>
Unannounced	<input type="checkbox"/>
Classification	
By	
Distribution	
Availability Code	
Avail Under Dist. Special	
A-1	

## 2. Cooccurrence matrices

### 2.1 Gray level cooccurrence

Given a vector  $\delta = (\Delta x, \Delta y)$  and a picture, we can estimate the joint probability density of the pairs of gray levels that occur at pairs of points separated by  $\delta$  by counting all such pairs of gray levels in the picture. If the picture has been quantized to  $m$  levels, the result is an  $m$  by  $m$  matrix, where entry  $(i, j)$  is the number of times gray levels  $i$  and  $j$  occur at separation  $\delta$ . In our experiments we will use the symmetric form of this matrix, i.e., we define the entries of the matrix  $M_\delta$  to be the numbers of times that pairs of gray levels occur at separation either  $\delta$  or  $-\delta$ .

When  $\delta$  is small compared to the texture element size, the high values in  $M_\delta$  are concentrated near the main diagonal. As  $\delta$  approaches texture element size, the gray levels of points will in general be quite different, so values will be more uniformly spread out in  $M_\delta$ . For example, Figure 2 shows the cooccurrence matrices derived from the pictures in Figure 1 for  $\delta = (0, 2)$ .

## 2.2 Edge maxima cooccurrence

Alternatively to measuring cooccurrence of pairs of gray levels, it has been suggested [3] that cooccurrence of other local properties, e.g., edge orientations at pairs of points with local maximum edge magnitudes, are useful texture measures. This class of cooccurrence matrices is computed as follows: first, a set of feature points is determined by applying non-maximum suppression to the output of a local operator on a picture. Next, a neighbor function is used to pair up these local maxima based on their relative locations and descriptions. Finally, the cooccurrence matrix  $G$  is computed by counting the pairs of descriptions associated with these pairs of points. That is,  $G(i,j)$  is the number of pairs that have descriptions  $i$  and  $j$ . If there are  $m$  possible descriptions associated with these local maxima, then  $G$  is  $m$  by  $m$ .

In this study we used as our local operator the magnitude of an edge detector based on differences of averages over 2 by 2 neighborhoods, and we used edge orientation as the descriptor. A point's edge magnitude is defined to be the maximum absolute difference of 2 by 2 blocks of pixels oriented in directions  $0^\circ$ ,  $45^\circ$ ,  $90^\circ$ , and  $135^\circ$ ; thus  $G$  is a 4 by 4 matrix. Non-maximum suppression was then applied in the direction normal to the direction of maximum edge response. Figure 3 shows the edge maxima computed from the textures in Figure 1.

Two neighbor functions were used here; they are similar to those in [3]. The first specifies a set of points,  $N_1$ , in an hourglass-shaped region centered at an edge maximum and oriented in the direction of the edge at that point; each triangular sector has angular width  $45^\circ$  and height 5. This set of points is shown in Figure 4a, where points labeled  $i$  are neighbors of the center point when its edge orientation is  $45i$ .  $G_{N_1}(i,j)$  is the number of times that an edge maximum with orientation  $j$  is a neighbor of an edge maximum with orientation  $i$ . We call  $G_{N_1}$  the edge maxima cooccurrence matrix for all neighbors along an edge.

The second neighbor function is also an hourglass-shaped region,  $N_2$ , of the same dimensions, but oriented in the direction perpendicular to the edge (Figure 4b). In this case, an edge maximum  $p$  is paired with each edge maximum  $q$  that occurs in the hourglass area centered at  $p$  and oriented across  $p$ 's edge. Thus  $G_{N_2}(i,j)$  is the number of times that the edge maximum with orientation  $j$  is a neighbor of one with orientation  $i$ . We call  $G_{N_2}$  the edge maxima cooccurrence matrix for all neighbors across an edge.

Measuring cooccurrence of edge orientations of a point and its neighbors in the edge direction should indicate properties of the curvature of texture element boundaries; if texture boundaries are smooth, then the values in  $G_{N_1}$  should be concentrated

near the main diagonal. Conversely, for a fine texture or a jagged-border coarse texture, maxima will not in general have the same edge orientation as their paired points, so the values in  $G_{N_1}$  will be more spread out. Figure 5a shows these cooccurrence matrices for the textures in Figure 1. The cooccurrence matrix produced by pairing edge maxima across the edges should also measure shape and density properties of texture elements. Figure 5b shows  $G_{N_2}$  matrices for the textures in Figure 1.

### 2.3 Gray level cooccurrence based on edge maxima

Gray level cooccurrence uniformly measures a fixed spatial relationship of gray-tones and therefore its usefulness depends on the adequacy of this "average" gray level dependence over all parts of a texture. Edge maxima cooccurrence measures edge orientation dependence, which captures texture element boundary properties, but ignores the tonal properties of these elements. We now define a new class of methods which measures the gray level cooccurrence of pairs of points at and near edge maxima. This hybrid scheme attempts to localize the measure of gray level spatial dependency at selected points of a texture and in selected directions. Features derived from these matrices will indicate properties of pairs of points with specified relationships to the locations and orientations of the texture's edge maxima.

As in edge maxima cooccurrence, an edge map is first computed by applying an edge detector and then suppressing non-maxima. For each edge orientation, a neighbor function is given which pairs points at and near an edge point. The cooccurrence matrix  $H$  gives the gray level cooccurrences of these pairs of points, where  $H(i,j)$  is the number of pairs of gray levels that occur at a specified displacement relative to the locations and orientations of edge maxima.

The edge detector used here is the same one described in Section 2.2, i.e., differences of 2 by 2 averages in four directions. We now define several neighbor functions and the resulting

matrices computed using them which may be useful in estimating joint gray level density near texture element boundaries. Let  $p$  be a point having non-zero edge magnitude and edge orientation  $\theta$ , and let  $d$  be a given distance.

a) Most similar neighbor along an edge.

Let  $q$  be the point at distance  $d$  from  $p$  in the  $\theta$  direction and let  $r$  be the point at distance  $d$  from  $p$  in direction  $\theta + \pi$ . Let  $i, j, k$  be the gray levels of points  $p, q, r$ , respectively. Increment  $H_{F_1}(i, j)$  if  $|i-j| = \min(|i-j|, |i-k|)$ ; otherwise, increment  $H_{F_1}(i, k)$ . Thus,  $H_{F_1}$  measures the gray level cooccurrences of edge points with their most similar (in terms of gray level) neighbors in the directions along their edges.

This matrix measures properties of the curvature of texture element boundaries. If boundaries are generally straight, then pairs of points will usually belong to the same population and high values will occur along the main diagonal of  $H_{F_1}$ . If the boundary turns frequently, then edge points will often be paired with points inside or outside a texture element depending on the direction of curvature. Figure 6a illustrates this definition for  $d=2$  for the textures in Figure 1.

b) Most similar neighbor across an edge.

Let  $q$  be the point at distance  $d$  from  $p$  in direction  $\theta + (\pi/2)$  and let  $r$  be the point at distance  $d$  from  $p$  in the  $\theta - (\pi/2)$  direction. Increment  $H_{F_2}(i, j)$  if  $|i-j| = \min(|i-j|, |i-k|)$ ;

otherwise increment  $H_{F_2}(i,k)$ . This method pairs each edge point with that point which is perpendicular to the edge's direction and has the most similar gray level to that of the given point. Thus each point is paired with a neighbor which is (presumably) inside the same texture element; features based on this matrix will reflect intra-region joint gray level probabilities of a texture's constituent elements. Figure 6b shows the method for  $d=2$ .

c) Least similar neighbor across an edge.

This method is the same as (b) except that we increment  $H_{F_3}(i,j)$  if  $|i-j|=\max(|i-j|,|i-k|)$ , and otherwise increment  $H_{F_3}(i,k)$ . This operation pairs points which are on opposite sides of an edge and therefore should measure joint gray level probability densities for adjacent texture elements. See Figure 6c.

d) Pair of neighbors across an edge.

This is also the same as (b), except that if  $q$  is the most similar point to  $p$ , then we increment  $H_{F_4}(j,l)$ , where  $l$  is the gray level of the point  $s$  which is at distance  $d$  from  $q$  in direction  $\theta+(\pi/2)$ . Similarly, if  $r$  is the most similar point to  $p$ , then we increment  $H_{F_4}(j,m)$ , where  $m$  is the gray level of the point  $t$  which is at distance  $d$  from  $r$  in direction  $\theta-(\pi/2)$ . Here, an edge point determines the direction of its interior and then continues in that direction to find another point. Thus

### 3. Experiments

A pilot study has been performed for preliminary evaluation of texture discriminability based on single features derived from the various cooccurrence matrices defined in Section 2. Subjective clustering criteria were used to evaluate performance (this is reasonable considering the size and dimensionality of the experiments).

Two sets of texture samples were used in the experiments. The first is a set of terrain samples selected from a LANDSAT image of eastern Kentucky and was used in [4]. Three representative images were chosen from each of the three geological terrain types, as shown in Figure 7a. A second data base was chosen from the Brodatz collection of textures [5]. Three windows of each of four texture types (the same types used in [6]) were chosen and are shown in Figure 7b. Both data sets were histogram flattened to remove any effects of unequal brightness and contrast in the originals. (One picture from each set was shown in Figure 1.)

The edge detector was, as mentioned earlier, the absolute difference of averages over 2 by 2 neighborhoods oriented in directions  $0^\circ$ ,  $45^\circ$ ,  $90^\circ$ , and  $135^\circ$ . Non-maximum suppression used a 1 by 4 neighborhood centered at the point of interest and oriented in the perpendicular direction to the edge. The output of this process for the two data bases is shown in Figure 8.

$H_{F_4}$  measures the joint gray level probability of pairs of interior points. See Figure 6d.

e) All neighbors along an edge.

Consider again the hourglass-shaped neighborhood of points,  $N_1$ , oriented in direction  $\theta$  at  $p$  as specified in Section 2.2. For each point  $q \in N_1$ , increment  $H_{F_5}(i, j)$ . This case is similar to (a); a set of cooccurrences is computed in the edge direction at each edge maximum. Again the joint probability density should be influenced by the shape characteristics of texture elements. Figure 6e illustrates this method.

f) All neighbors across an edge.

This is the same as (e) except that the hourglass neighborhood  $N_2$ , oriented across the edge, is used. Examples of this matrix,  $H_{F_6}$ , are shown in Figure 6f.

Four features, originally defined by Haralick [7], were computed from each normalized cooccurrence matrix (i.e., given matrix  $M$ , define  $p(i,j) = M(i,j)/\sum_{k,l} M(k,l)$ ):\*

$$1) \text{ Contrast (CON)} \equiv \sum_i \sum_j (i-j)^2 p(i,j)$$

$$2) \text{ Angular second moment (ASM)} \equiv \sum_i \sum_j p(i,j)^2$$

$$3) \text{ Entropy (ENT)} \equiv -\sum_i \sum_j p(i,j) \log p(i,j)$$

$$4) \text{ Correlation (COR)} \equiv \sum_i \sum_j [ijp(i,j) - \mu_x \mu_y] / (\sigma_x \sigma_y), \text{ where}$$

$\mu_x$  and  $\sigma_x$  are the mean and standard deviation of the row sums of the cooccurrence matrix, and  $\mu_y$  and  $\sigma_y$  are analogous statistics of the column sums.

The set of feature values derived using a given data set, cooccurrence matrix method and feature type, were plotted along a line with each window's value uniquely designated. Subjective evaluation of a feature was based on the visual separability of the texture classes in this plot.

After preliminary experiments using different values of  $\delta$  (distances 1, 2, 4 and directions 0, 45, 90, 135), it was found that individual features based on  $\delta=(0,2)$  did at least as well as features based on the other separations. These values have been plotted in Figures 9a and 10a for the Kentucky and Brodatz

---

\* In the case of the edge maximum cooccurrence matrices, matrix indices 1, 2, 3, 4 correspond to edge directions 90°, 0°, 45°, and 135°, respectively.

data bases respectively. In particular, the contrast and correlation features for the Kentucky samples are seen to group the three classes into well separable clusters. For the Brodatz textures, none of the features were very successful.

Edge maxima cooccurrence based features were computed for the two methods described above, namely all neighbors across an edge and all neighbors along an edge. These results are shown in Figures 9b,c and 10b,c. These features did not do well in distinguishing the terrain types, but the correlation feature for neighbors across an edge separated the four Brodatz textures. A partial explanation of these results can be derived by examining the edge maxima shown in Figure 8. This class of methods depends on the reliability and distinguishability of these thinned edge maps; if the edge maps associated with different features are not very different, then we would expect features based on the methods to be less successful. Here, the terrain edge maps are not very distinguishable and produce poor results, while the Brodatz texture edge maps can be visually discriminated.

The same features were computed for each of the six methods for measuring gray level cooccurrence near edge maxima. Distance  $d=2$  was used in each case. Figures 9d-i and 10d-i show the plotted values. The results on the Kentucky data were uniformly poor in separating the three terrain classes. Using the Brodatz samples, however, good separability was obtained using the entropy feature on each of the six matrices. This class of methods also

suffers when the thinned edge maps are not sufficiently different to distinguish the textures; in these cases it seems that other information than that found near edges is needed. In addition, these methods are based on the assumption that textures are describable as collections of primitive elements, so that edge maxima will correspond to points on the boundaries of these elements. The Brodatz textures fit this model and the results are successful; the terrain textures are wrinkled and contain line-like elements and consequently the methods used here are not the most appropriate ones.

Tables 1 and 2 summarize the results of Figures 9 and 10, respectively.

Cooccurrence Type	Method	Feature			
		ASM	CON	ENT	COR
Gray level	$\delta = (0, 2)$	B/A, C	A/B/C	B/A, C	A/B/C
	Along edge	poor	poor	poor	A/B
Edge maxima	Across edge	poor	poor	poor	A/B
	Most similar neighbor along edge	poor	poor	poor	poor
	Most similar neighbor across edge	poor	B/C	poor	poor
Gray level at and near edge maxima	Least similar neighbor across edge	poor	B/C	poor	poor
	Pair of neighbors across edge	poor	poor	poor	C/A, B
	All neighbors along edge	poor	poor	poor	A/B
	All neighbors across edge	poor	poor	poor	poor

Table 1. Summary of Figure 9 plots describing the separability of the terrain textures. A, B, C denote the three terrain classes; slash means "separated".

#### 4. Conclusion

A new class of cooccurrence matrices has been defined which measures the joint occurrences of gray levels at pairs of points at locations and separations defined relative to the positions and orientations of edge maxima. This selective cooccurrence approach is not likely to be sensitive to the size of texture elements as is the standard gray level cooccurrence method. Experimental results on a small number of coarse textures, though not statistically significant, appear to show a marked improvement in the features based on gray level cooccurrence near edge maxima over features based on fixed separation gray level cooccurrence.

Cooccurrence Type	Method	Feature			
		ASM	CON	ENT	COR
Gray level	$\delta = (0, 2)$	W/G, R, S	G/W/R, S	G/W/R, S	G/W/R, S
Edge maxima	Along edge	W/R, S	R/S/G, W	W/G, R, S	G/R/S, W
	Across edge	poor	R/W/G, S	W/G, S	R/G, S, W
Gray level at and near edge maxima	Most similar neighbor along edge	R/G	poor	G/R/S/W	R/G, S
	Most similar neighbor across edge	R/G	poor	G/R/S/W	R/S, W
	Least similar neighbor across edge	R/G	G, S/R, W	G/R/S/W	G/R/W
	Pair of neighbors across edge	G, S/R, W	W/G, S	G/R/S/W	R/G, S, W
	All neighbors along edge	G/R/W	W/G, S	G/R/S/W	G, S/R, W
	All neighbors across edge	G/R	G/R, W	G/R/S/W	G/R, W

Table 2. Summary of Figure 10 plots describing the separability of the Brodaz textures. G = grass, R = raffia, S = sand, W = wool; slash means "separated".

2	
3 2 2 2 1	
3 3 3 2 2 2 1 1 1	
3 3 3 2 1 1 1	
0 0 3 3 2 1 1 0 0	
0 0 0 0 0 X 0 0 0 0 0	
0 0 1 1 2 3 3 0 0	
1 1 1 2 3 3 3	
1 1 1 2 2 2 3 3 3	
1 2 2 2 3	

a.

0	
1 0 0 0 3	
1 1 1 0 0 0 3 3 3	
1 1 1 0 3 3 3	
2 2 1 1 0 3 3 2 2	
2 2 2 2 2 X 2 2 2 2 2	
2 2 3 3 0 1 1 2 2	
3 3 3 0 1 1 1	
3 3 3 0 0 0 1 1 1	
3 0 0 0 1	

b.

Figure 4. Edge maxima at points labeled  $i$  are paired with the point  $x$  when  $x$ 's edge orientation is  $45i^\circ$ .

- (a) Neighbor function  $N_1$  for all points along an edge.
- (b) Neighbor function  $N_2$  for all points across an edge.

	$0^\circ$	$45^\circ$	$90^\circ$	$135^\circ$
$0^\circ$	84	145	110	206
$45^\circ$	180	911	399	329
$90^\circ$	73	492	212	387
$135^\circ$	169	327	394	900

Terrain

a.

	$0^\circ$	$45^\circ$	$90^\circ$	$135^\circ$
$0^\circ$	41	109	42	74
$45^\circ$	171	1211	256	423
$90^\circ$	12	393	58	198
$135^\circ$	166	368	137	343

Raffia

	$0^\circ$	$45^\circ$	$90^\circ$	$135^\circ$
$0^\circ$	35	131	73	118
$45^\circ$	109	444	235	327
$90^\circ$	110	395	266	373
$135^\circ$	116	329	258	436

Terrain

b.

	$0^\circ$	$45^\circ$	$90^\circ$	$135^\circ$
$0^\circ$	28	100	12	72
$45^\circ$	84	555	148	367
$90^\circ$	42	292	126	192
$135^\circ$	52	422	115	270

Raffia

Figure 5. Edge maxima cooccurrence matrices for Figure 1 textures. (a)  $G_{N_1}$  matrix for all neighbors along an edge.

- (b)  $G_{N_2}$  matrix for all neighbors across an edge.



Figure 1. A LANSAT terrain texture and the raffia texture from Brodatz [5].

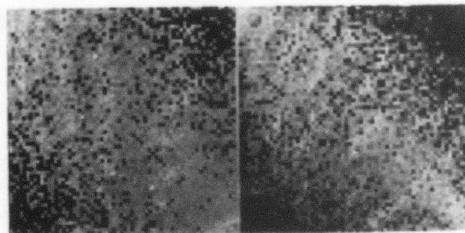
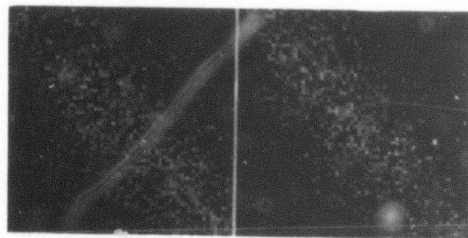


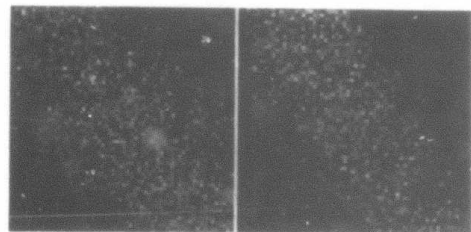
Figure 2. Gray level cooccurrence matrices  $M_{(0,2)}$  for the textures in Figure 1. Each entry's value was scaled by  $1n32$  and displayed as a 2 by 2 block for visibility.



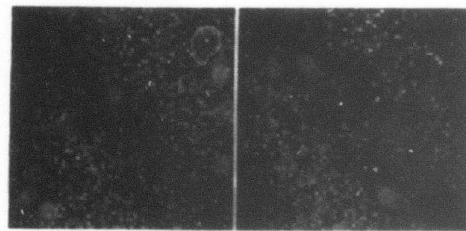
Figure 3. Edge maxima after non-maximum suppression for pictures in Figure 1. (Thresholded for visibility.)



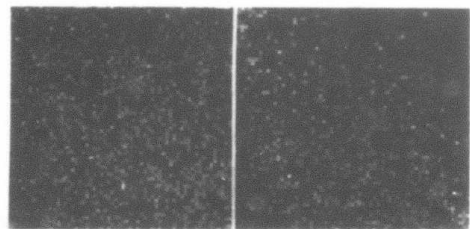
a.



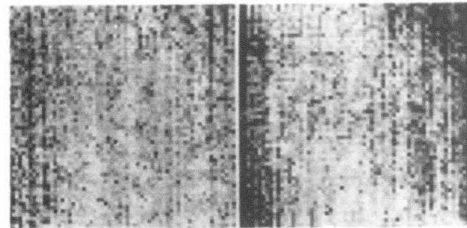
b.



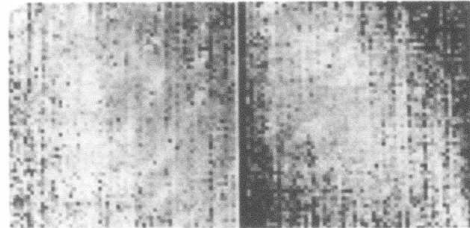
c.



d.

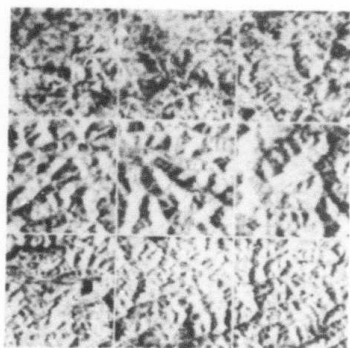


e.

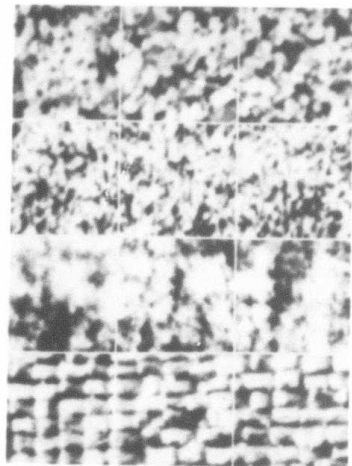


f.

Figure 6. Gray level cooccurrence matrices based on edge maxima for textures in Figure 1. a-f correspond to matrices  $H_{F1}$ - $H_{F6}$ . Each entry's value was scaled by  $\ln 32$ .



a.

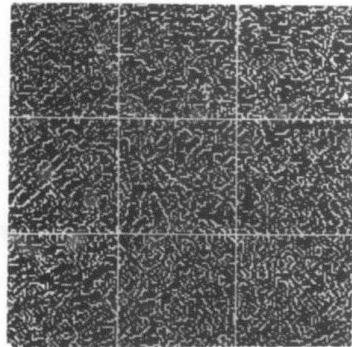


b.

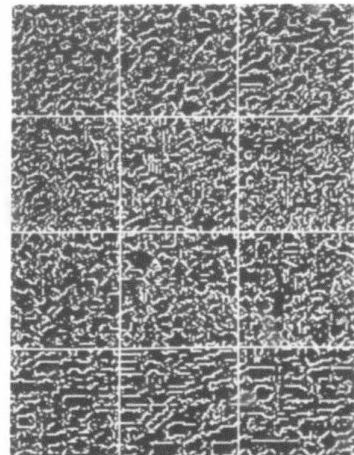
Figure 7. Data bases after histogram flattening.

(a) LANDSAT terrain samples. Top row is Mississippian limestone and shale, second row is Pennsylvanian sandstone and shale, and third row is Lower Pennsylvanian shale.

(b) Brodatz textures. Top row is sand (plate D29), second row is grass (D9), third row is wool (D19), and fourth row is raffia (D84).



a.



b.

Figure 8. Edge maxima after non-maximum suppression for textures in Figure 7. (Thresholded for visibility.)

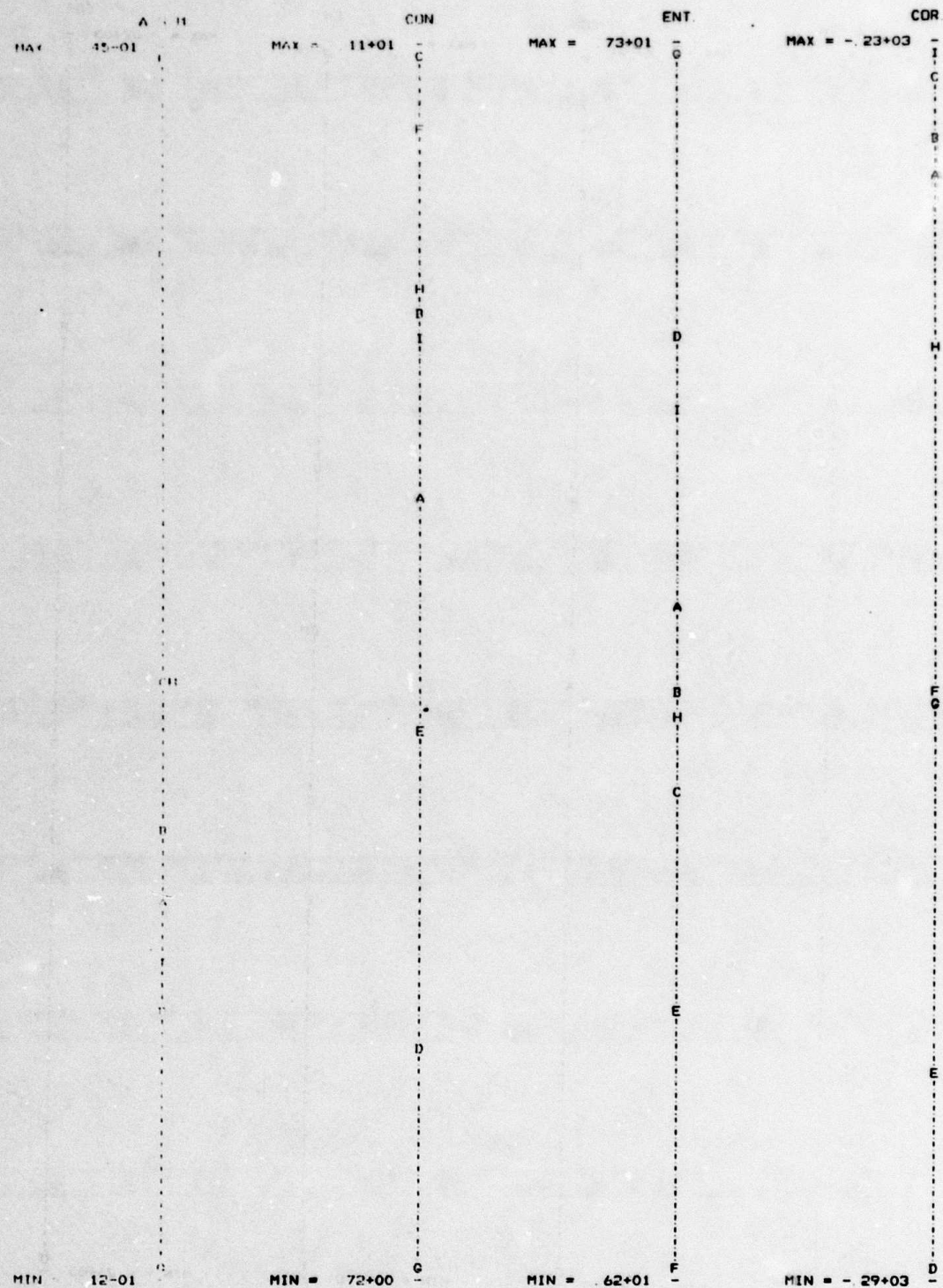


Figure 9b. Features derived from  $G_{N_1}$  for terrain samples.

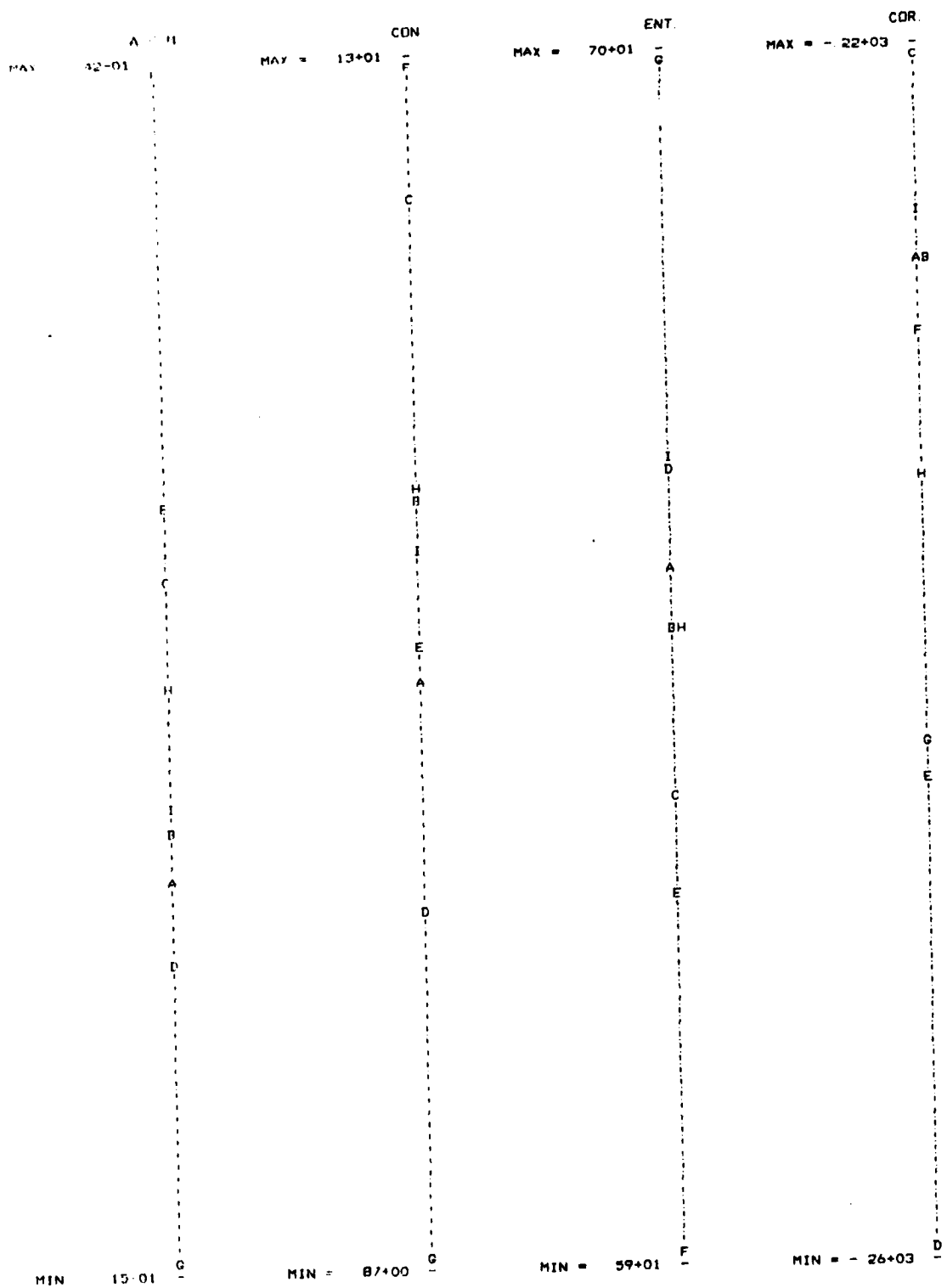


Figure 9c. Features derived from  $G_{N_2}$  for terrain samples.

Figure 9d. Features derived from  $H_{F_1}$  for terrain samples.

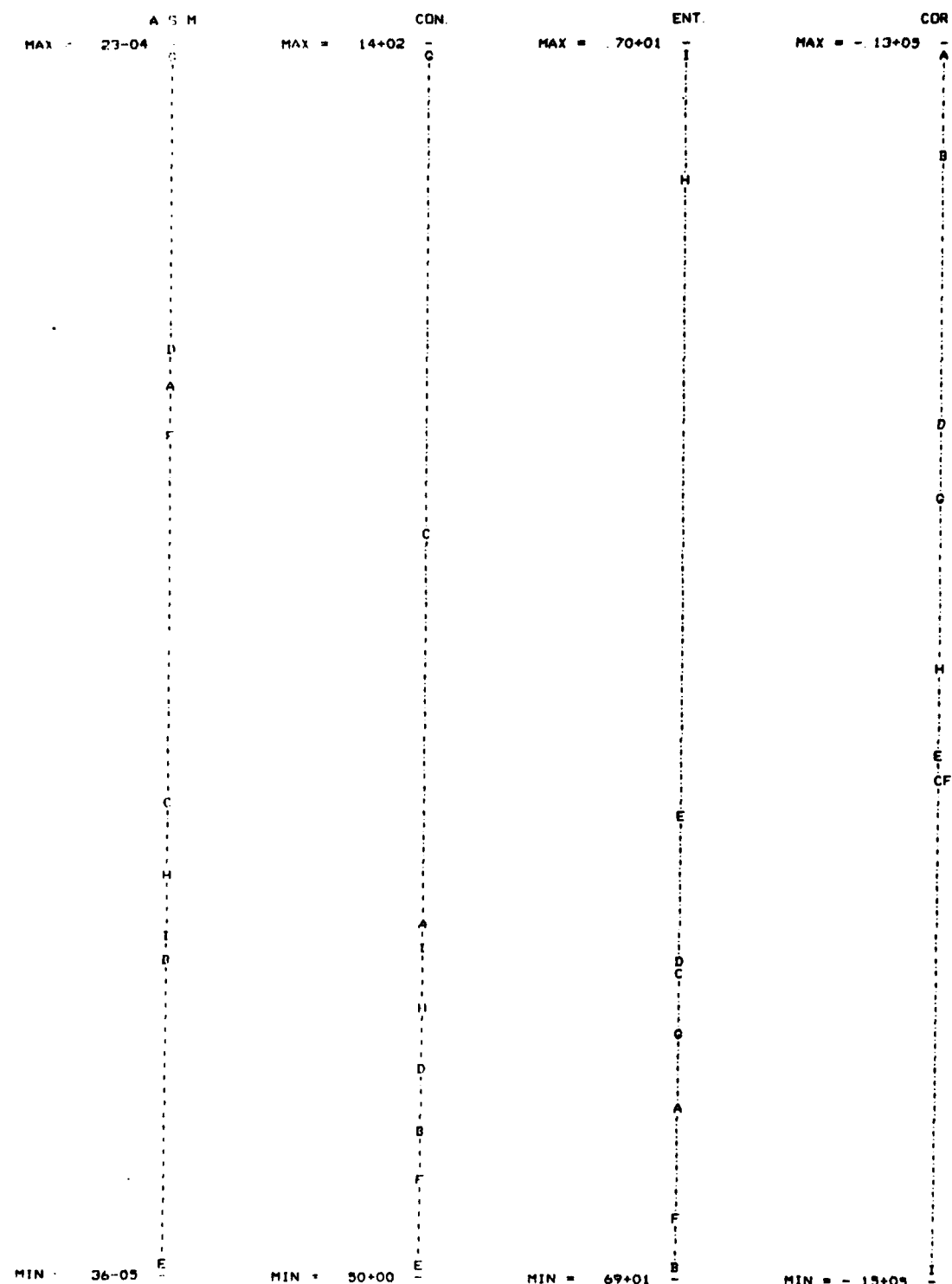


Figure 9e. Features derived from  $H_{F_2}$  for terrain samples.

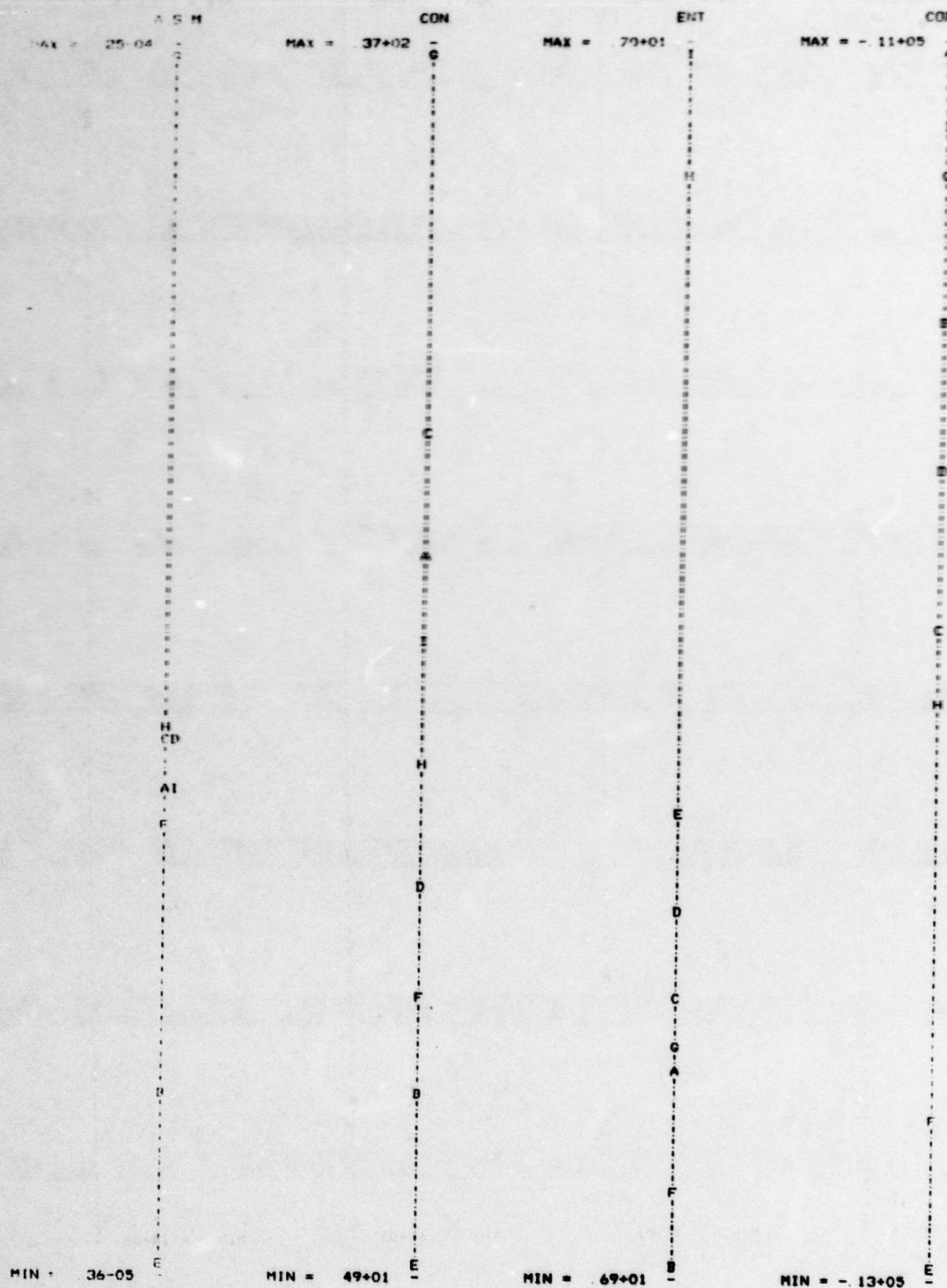


Figure 9f. Features derived from  $H_{F_3}$  for terrain samples.

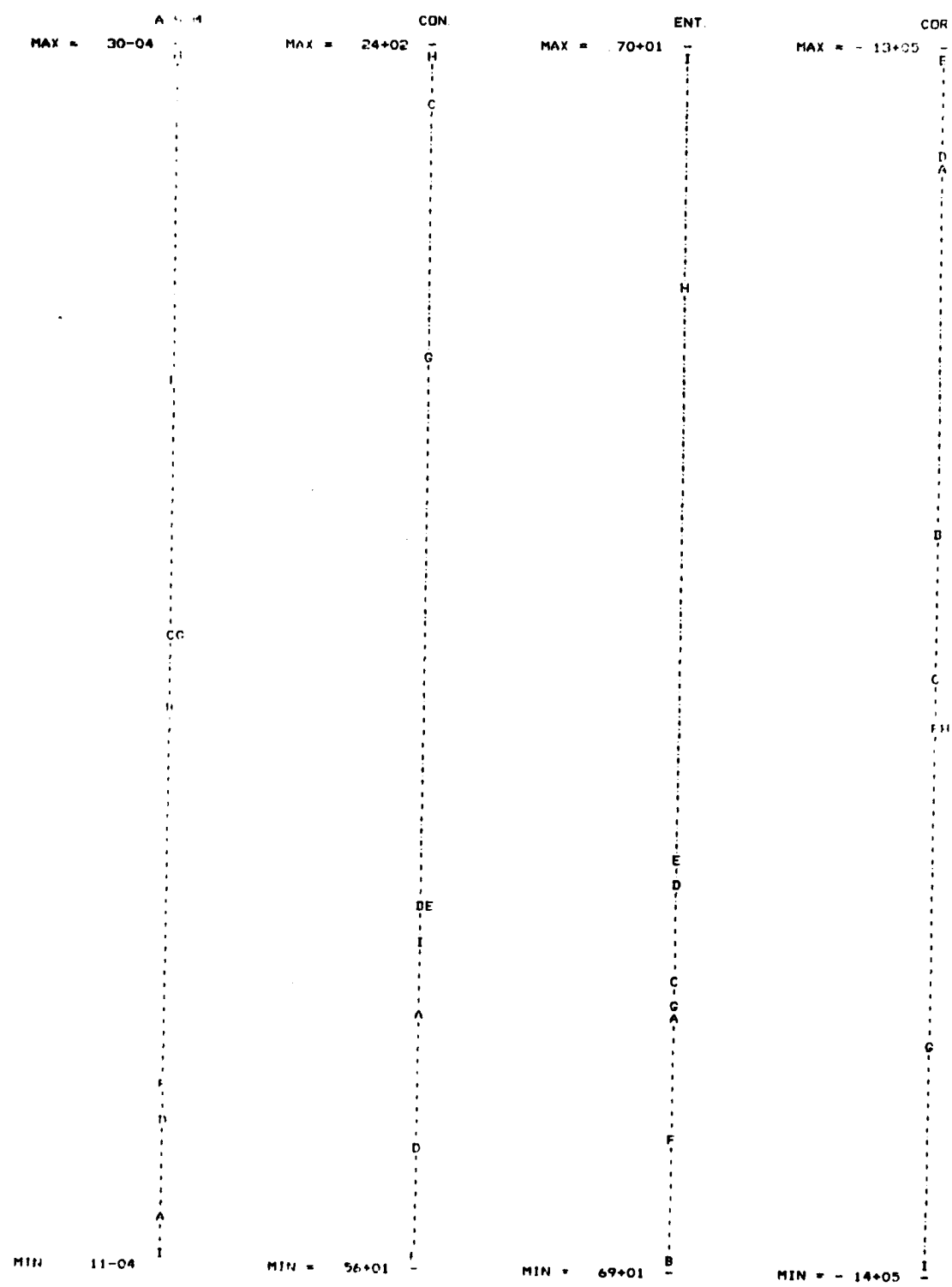


Figure 9g. Features derived from  $H_{F_4}$  for terrain samples.

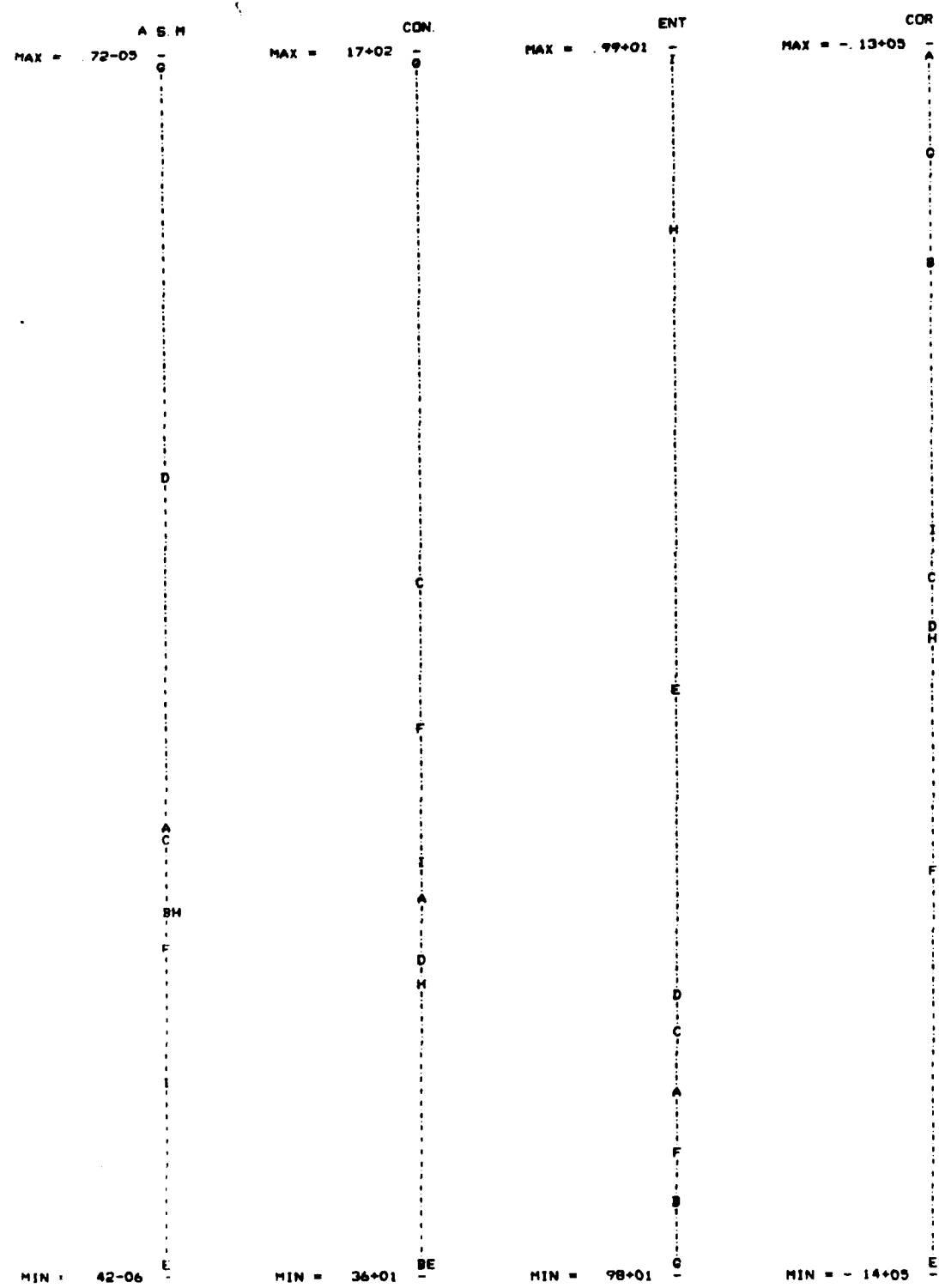


Figure 9h. Features derived from  $H_{F5}$  for terrain samples.

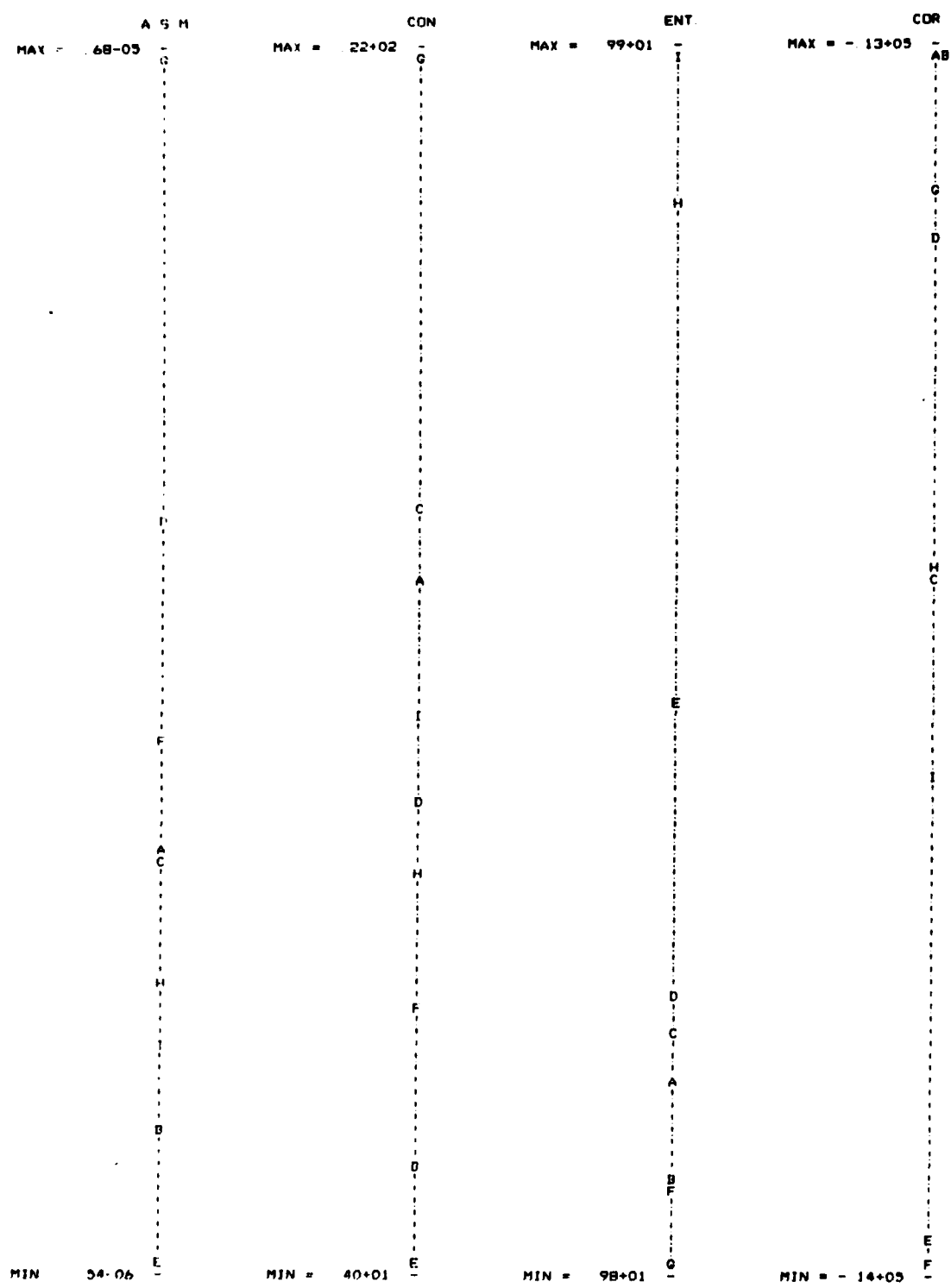
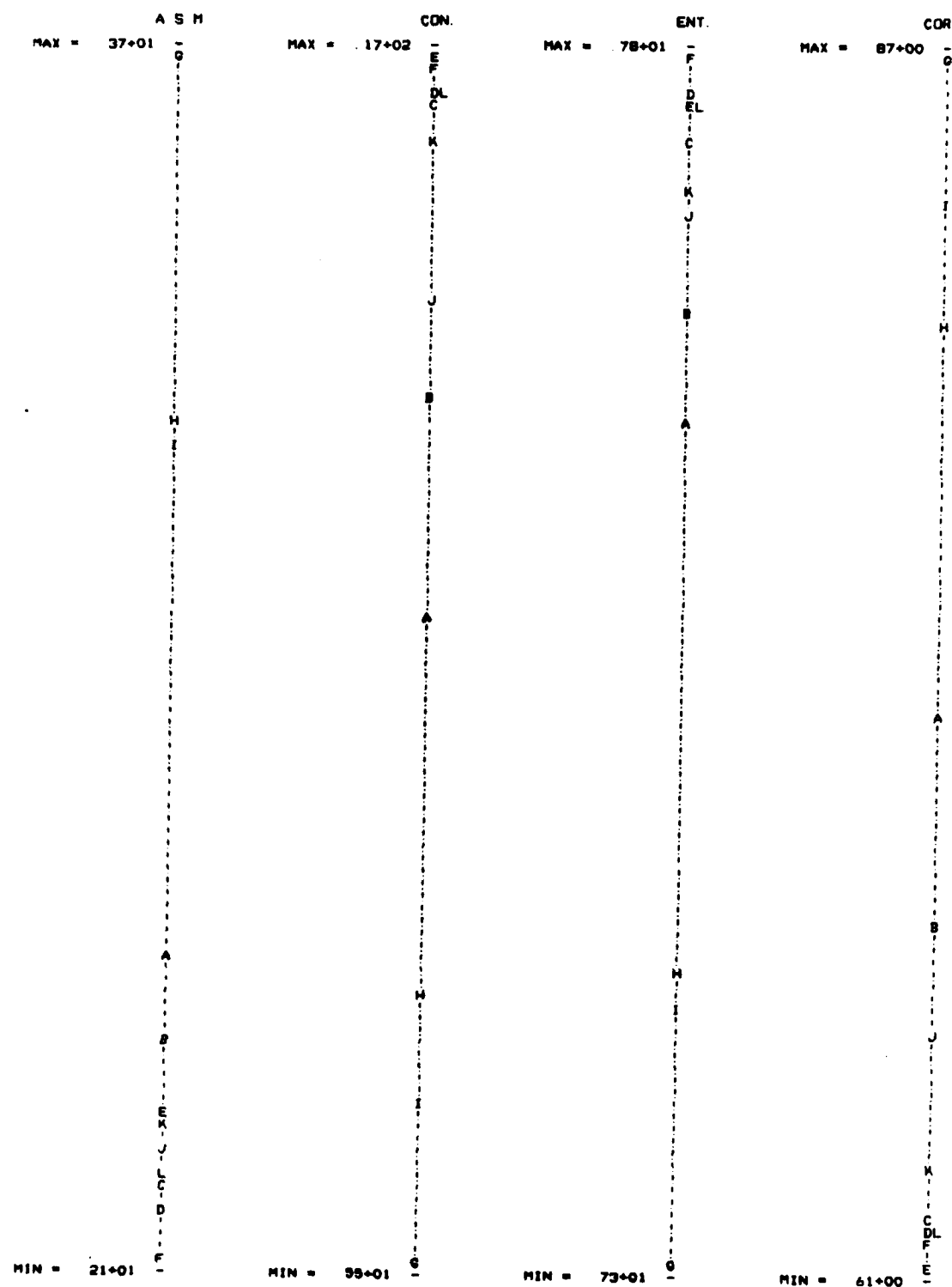


Figure 9i. Features derived from  $H_{F_6}$  for terrain samples.



a. Features derived from  $M_{(0,2)}$  for Brodatz textures.

**Figure 10.** Feature plots of ASM, CON, ENT and COR derived using the nine cooccurrence matrix methods described in Section 2 for the Brodatz texture samples in Figure 7b. Labels A-C denote the sand windows, D-F denote grass, G-I denote wool, and J-L denote raffia.

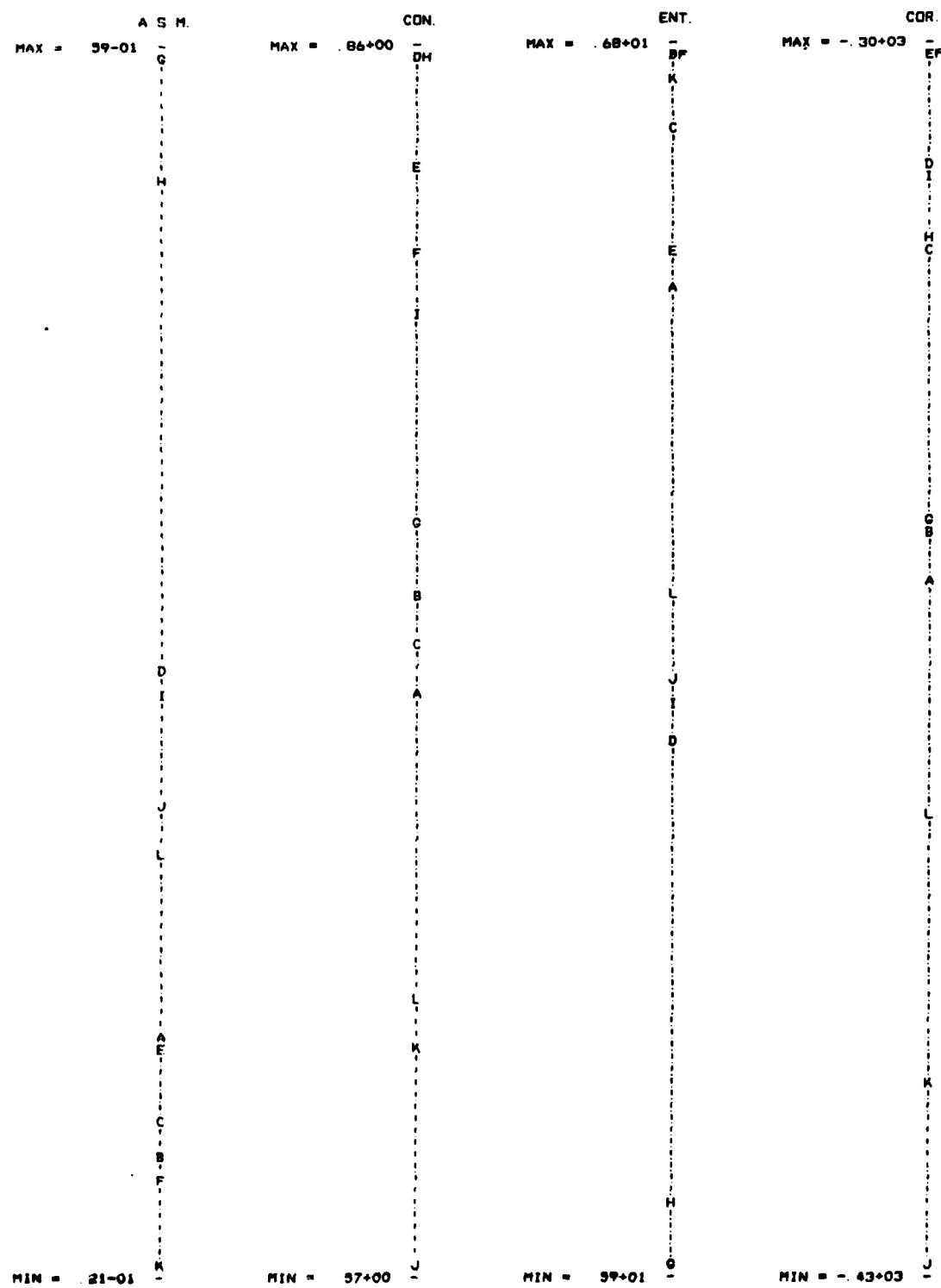


Figure 10b. Features derived from  $G_{N_1}$  for Brodatz textures.

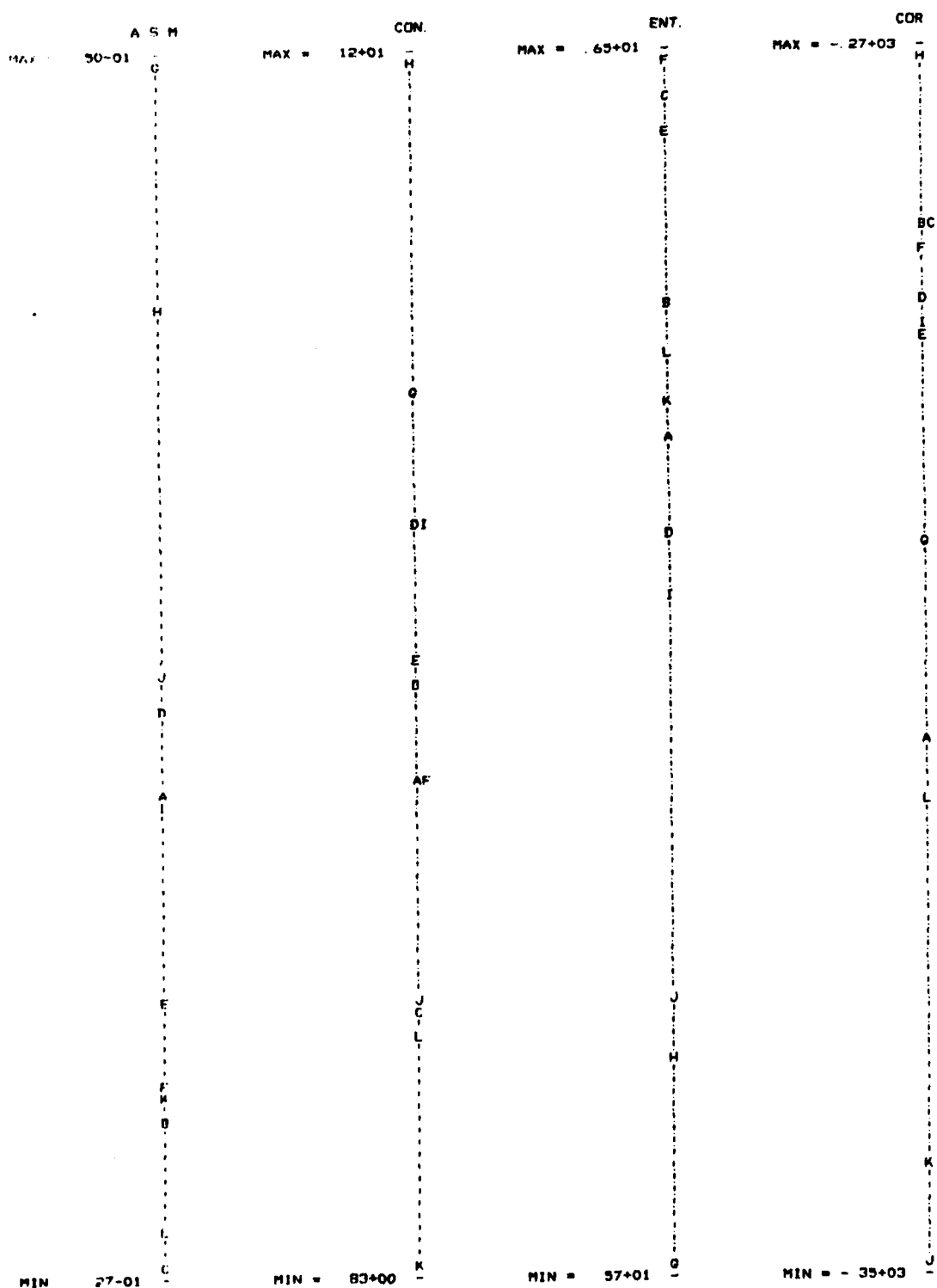


Figure 10c. Features derived from  $G_{N_2}$  for Brodatz textures.

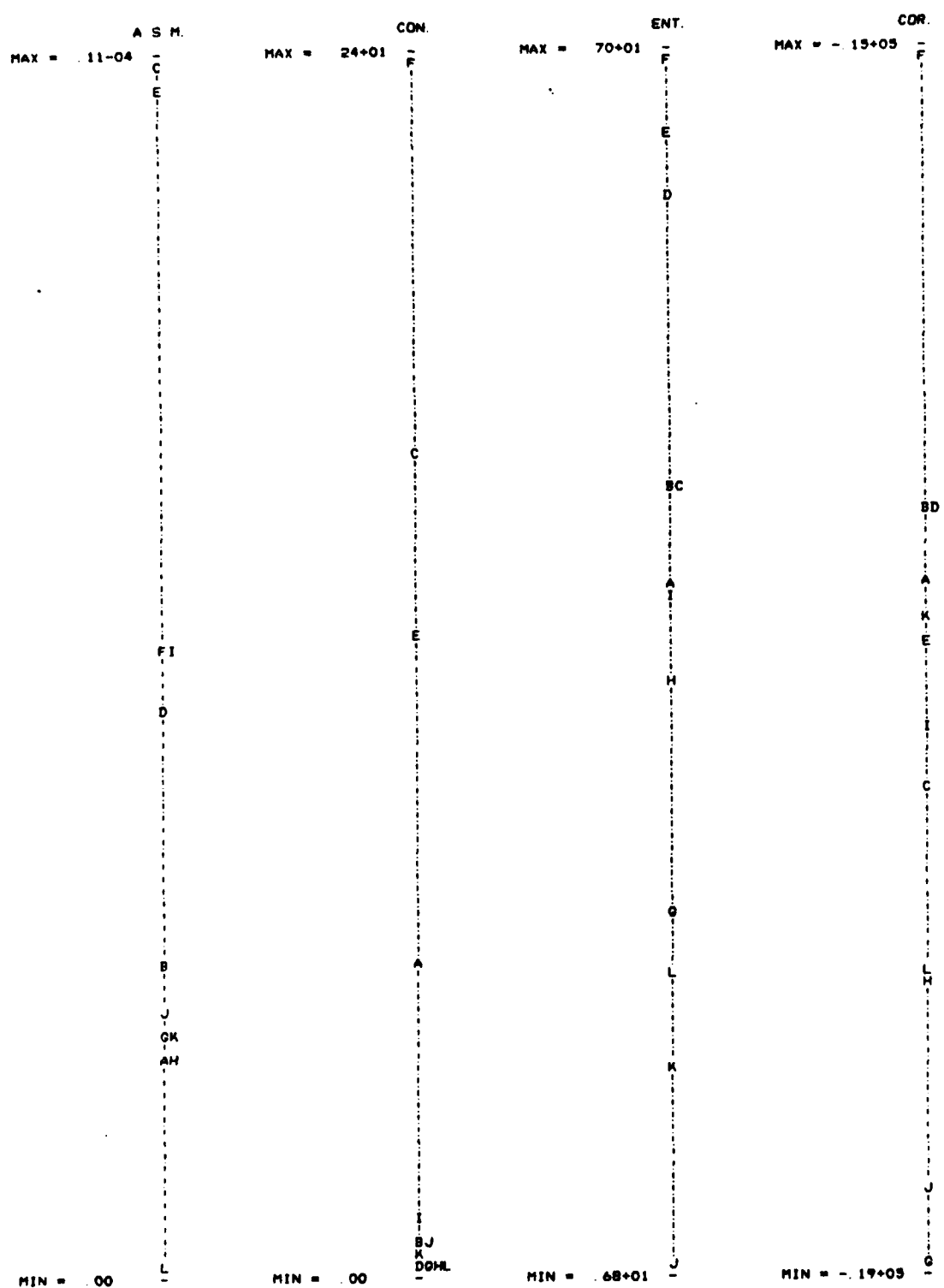


Figure 10d. Features derived from  $H_{F_1}$  for Brodatz textures.

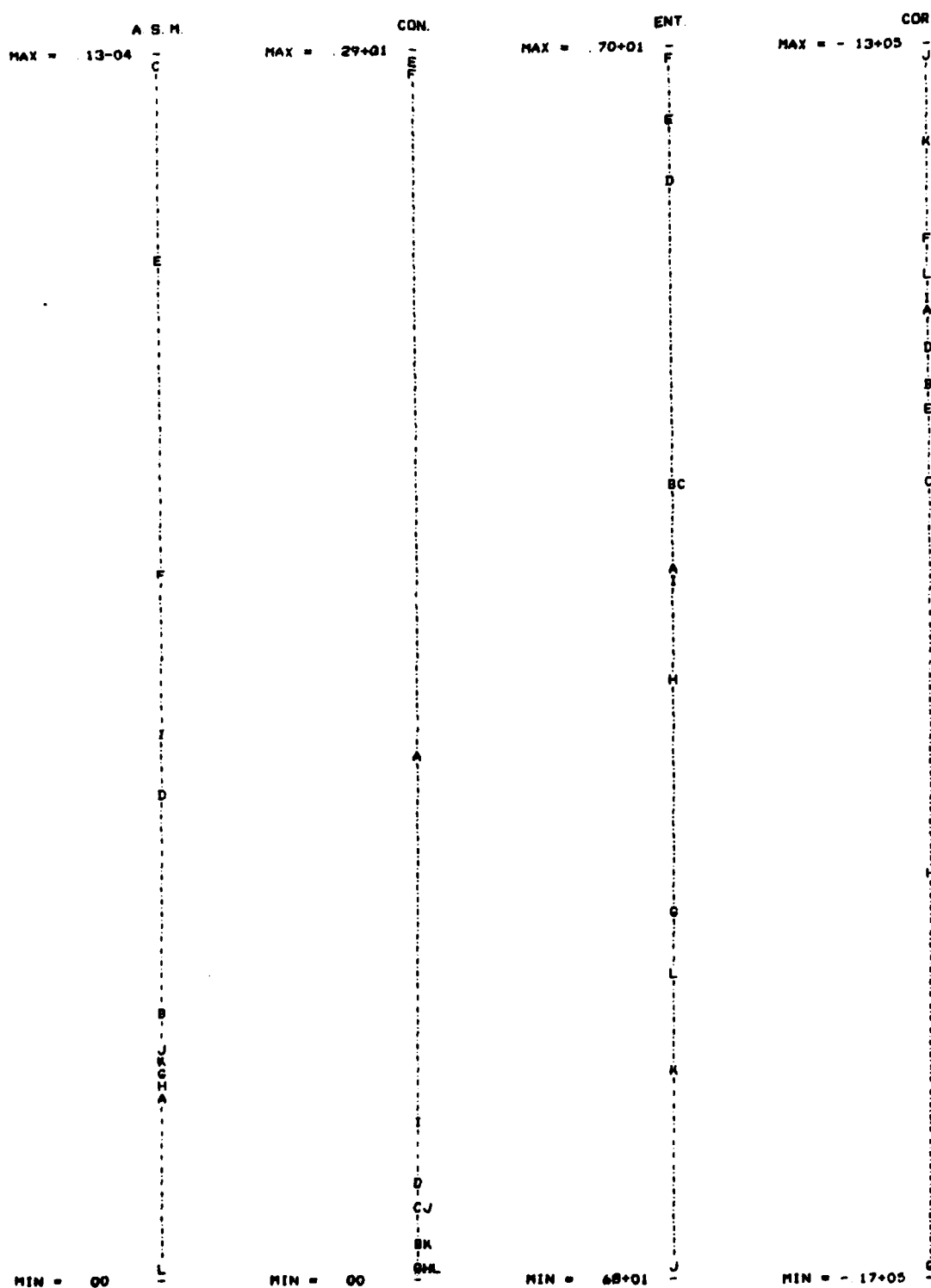


Figure 10e. Features derived from  $H_{P_2}$  for Brodatz textures.

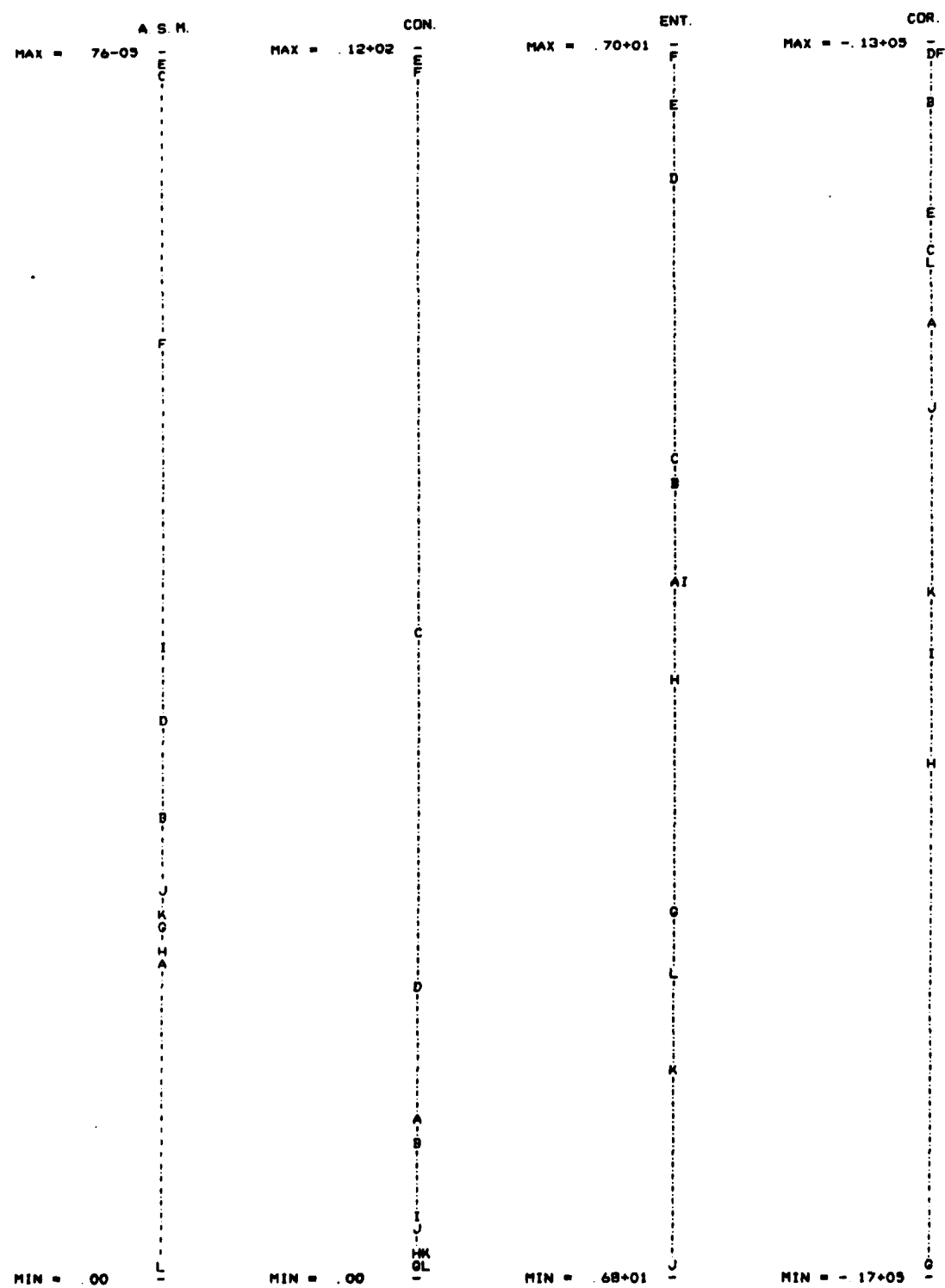


Figure 10f. Features derived from  $H_{F_3}$  for Brodatz textures.

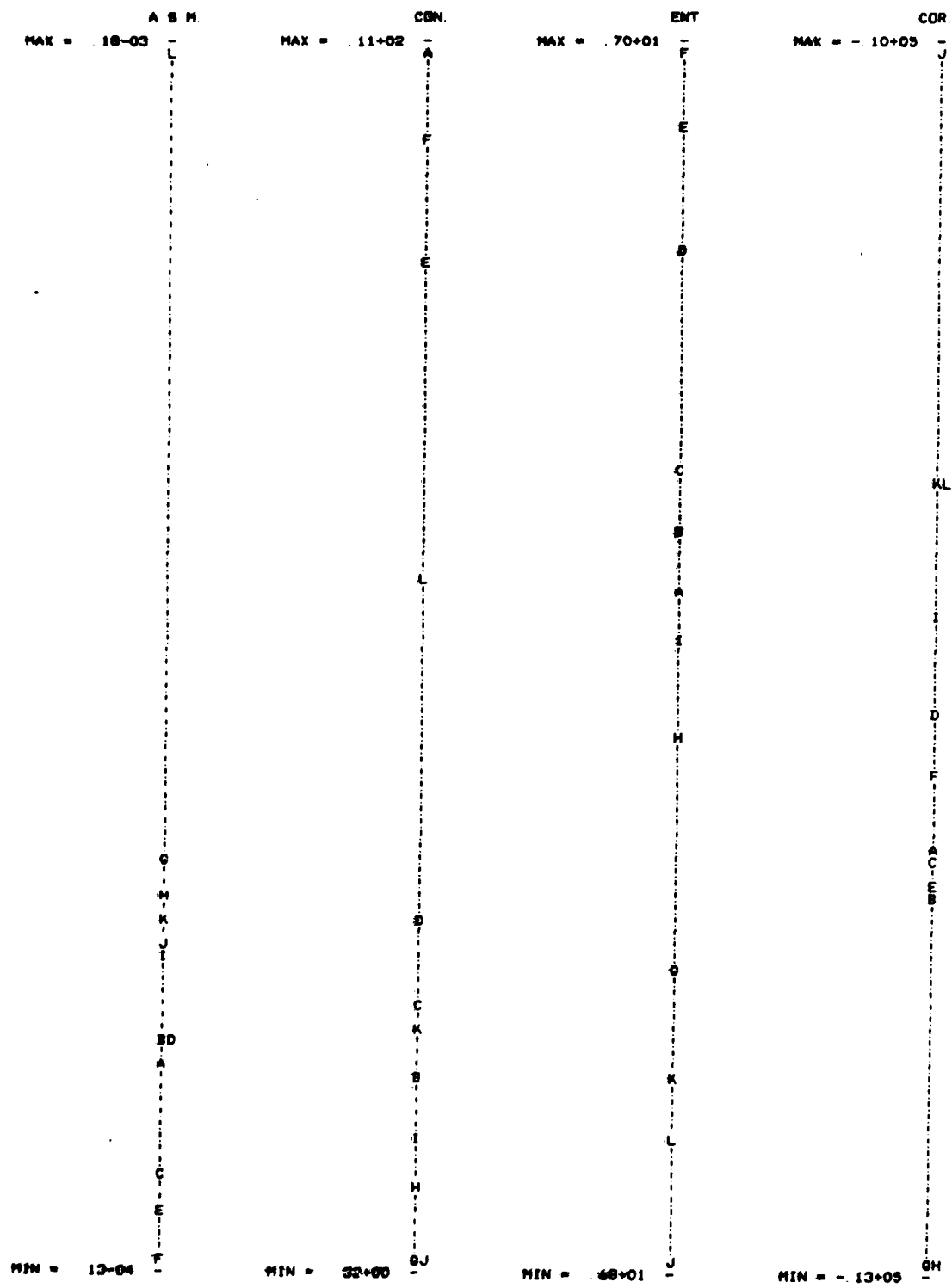


Figure 10g. Features derived from  $H_{F_4}$  for Brodatz textures.

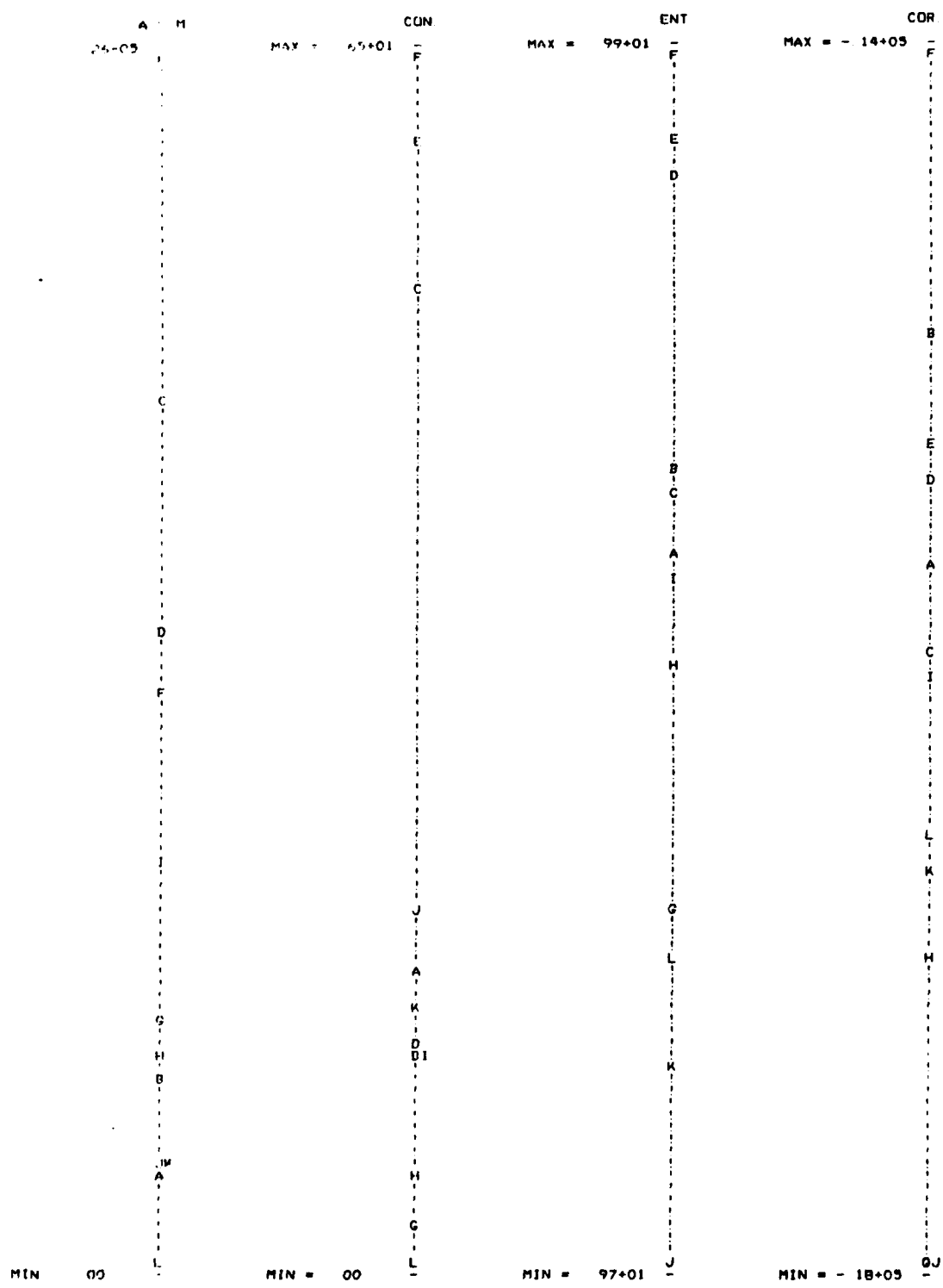


Figure 10h. Features derived from  $H_{F_5}$  for Brodatz textures.

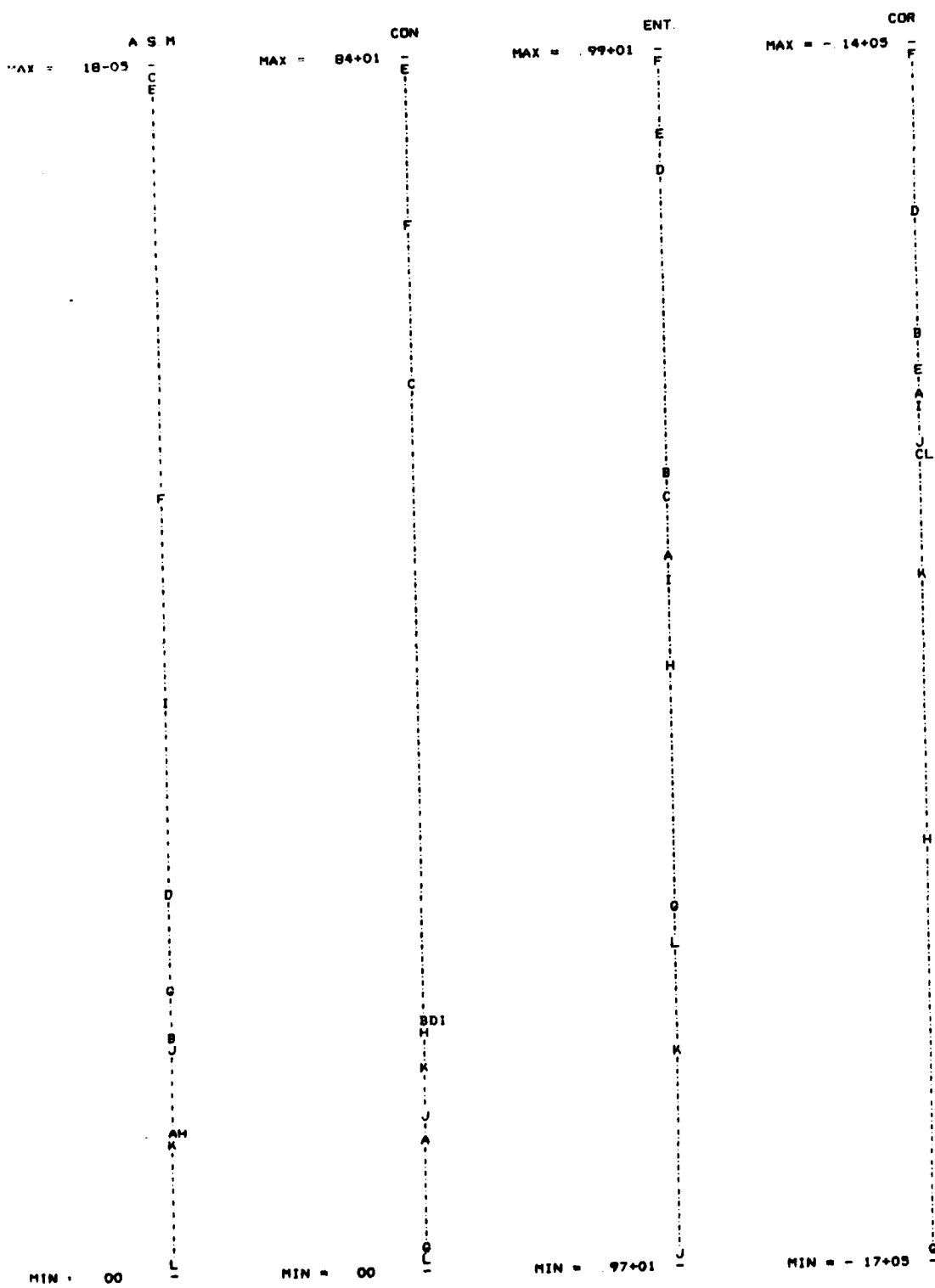


Figure 10i. Features derived from  $H_{F_6}$  for Brodatz textures.

### References

1. R. M. Haralick, Statistical and structural approaches to texture, Proc. 4th International Joint Conference on Pattern Recognition, 1978, 45-68.
2. L. Davis, S. Johns, and J. K. Aggarwal, Texture analysis using generalized cooccurrence matrices, Proc. IEEE Conf. on Pattern Recognition and Image Processing, 1978, 313-318.
3. L. Davis, S. Johns, and J. K. Aggarwal, Texture analysis using generalized cooccurrence matrices, preprint.
4. J. S. Weszka, C. R. Dyer, and A. Rosenfeld, A comparative study of texture measures for terrain classification, IEEE Trans. Systems, Man, and Cybernetics SMC-6, 1976, 269-285.
5. P. Brodatz, Textures, Dover, New York, 1966.
6. W. K. Pratt, Quantitative design and evaluation methods for edge and texture feature extraction, Proc. Image Understanding Workshop, Nov. 1978, 103-109.
7. R. M. Haralick, K. Shanmugam, and I. Dinstein, Textural features for image classification, IEEE Trans. Systems, Man, and Cybernetics SMC-3, 1973, 610-621.

**Unclassified**

SECURITY CLASSIFICATION OF THIS PAGE (When Data Entered)

REPORT DOCUMENTATION PAGE		READ INSTRUCTIONS BEFORE COMPLETING FORM
1. REPORT NUMBER	2. GOVT ACCESSION NO.	3. RECIPIENT'S CATALOG NUMBER
4. TITLE (and Subtitle) <b>Texture Classification Using Gray Level Cooccurrence Based on Edge Maxima</b>		5. TYPE OF REPORT & PERIOD COVERED <b>Technical</b>
7. AUTHOR(s) <b>Charles R. Dyer, Tsai-Hong Hong, and Azriel Rosenfeld</b>		6. PERFORMING ORG. REPORT NUMBER <b>TR-738</b>
8. PERFORMING ORGANIZATION NAME AND ADDRESS <b>Computer Science Center University of Maryland College Park, MD 20742</b>		9. CONTRACT OR GRANT NUMBER(s) <b>DAAG-53-76C=0138</b>
11. CONTROLLING OFFICE NAME AND ADDRESS <b>U. S. Army Night Vision Laboratory Fort Belvoir, VA 22060</b>		10. PROGRAM ELEMENT, PROJECT, TASK AREA & WORK UNIT NUMBERS
14. MONITORING AGENCY NAME & ADDRESS(if different from Controlling Office)		12. REPORT DATE <b>March 1979</b>
		13. NUMBER OF PAGES <b>40</b>
16. DISTRIBUTION STATEMENT (of this Report)  <b>Approved for public release; distribution unlimited</b>		15. SECURITY CLASS. (of this report) <b>Unclassified</b>
17. DISTRIBUTION STATEMENT (of the abstract entered in Block 20, if different from Report)		
18. SUPPLEMENTARY NOTES		
19. KEY WORDS (Continue on reverse side if necessary and identify by block number)  <b>Image processing, and Pattern recognition, <u>A</u> Texture analysis.</b>		
20. ABSTRACT (Continue on reverse side if necessary and identify by block number)  <b>This paper introduces a new class of texture features, based on the joint occurrences of gray levels at points defined relative to edge maxima. These features are compared with previous types of cooccurrence-based features, and experimental results are presented indicating that the new features should be useful for texture classification.</b> <i>Originator-supplied Keywords include:</i>		

Blank

Page